

Total Structural Determination of $[\text{Au}_1\text{Ag}_{24}(\text{Dppm})_3(\text{SR})_{17}]^{2+}$ Comprised by An Open Icosahedral $\text{Au}_1\text{Ag}_{12}$ Core with Six Free Valence Electrons

Yangfeng Li,^{a,‡} Manman Zhou,^{a,‡} Shan Jin,^{b,*} Lin Xiong,^c Qianqin Yuan,^a Wenjun Du,^a Yong Pei,^{c,*}
Shuxin Wang,^a Manzhou Zhu^{a,b,*}

a. Department of Chemistry and Centre for Atomic Engineering of Advanced Materials, Anhui Province, Key Laboratory of Chemistry for Inorganic/Organic Hybrid Functionalized Materials, Anhui University, Hefei, Anhui, 230601, P. R. China

b. Institute of Physical Science and Information Technology, Anhui University, Hefei, Anhui, 230601, P. R. China

c. Department of Chemistry, Key Laboratory of Environmentally Friendly Chemistry and Applications of Ministry of Education, Xiangtan University, Hunan Province, China, 411105, P.R. China

1.1 Chemicals Materials

Tetrachloroauric(III) acid ($\text{HAuCl}_4 \cdot 3\text{H}_2\text{O}$, 99.99%), silver nitrate (AgNO_3 , 99.0%, Sigma-Aldrich), Borane-tert-butylamine complex (97%, Energy Chemical), bis-(diphenylphosphino)methane (Dppm, 98%), Cyclohexyl mercaptan ($\text{C}_6\text{H}_{12}\text{S}$, 97%), Tetraphenylboron sodium (NaBPh_4 , 98%), Tetraphenylphosphonium bromide (PPh_4Br , 98%), 2,4-Dimethylbenzenethiol (HSPHMe_2 , 96%), methanol (CH_3OH , HPLC, Aldrich), n-hexane (Hex, HPLC grade, Aldrich), dichloromethane (CH_2Cl_2 , HPLC grade, Aldrich). All reagents were used as received without further purification.

1.2 The Synthesis of $[\text{Au}_1\text{Ag}_{24}(\text{Dppm})_3(\text{SR})_{17}]^{2+}$

Typically, gold salt ($\text{HAuCl}_4 \cdot 3\text{H}_2\text{O}$, 20 mg, 0.05 mmol) and AgNO_3 (40 mg, 0.235 mmol, dissolved in 2 ml CH_3OH) were added to 20 ml CH_3OH under vigorous stirring. After 10 mins, bis-(diphenylphosphino)methane (Dppm, 50 mg, 0.13 mmol) and cyclohexylmercaptan ($\text{C}_6\text{H}_{12}\text{S}$, 50 μl , 0.40 mmol) were added together to the mixed solution. After 20 min, a freshly prepared solution of borane-tert-butylamine complex (50 mg, in 2 ml CH_3OH) was added. The reaction lasted for 12 h at room temperature. The crude product was obtained by centrifugation (5 min at ~ 10000 rpm). The product was washed by methanol three times. Later, the as-obtained alloy cluster was dissolved in 1 ml CH_2Cl_2 and NaBPh_4 (30 mg, 0.088 mmol) in 3 ml CH_3OH was added to replace the anion of the cluster for easy crystallization. The precipitate was collected by centrifugation (5 min at ~ 10000 rpm). The precipitate was washed by methanol two times and collected by centrifugation again. Red crystals were crystallized from CH_2Cl_2 /hexane three times later at room temperature.

1.3 The Synthesis of $\text{Au}_1\text{Ag}_{24}(\text{SPhMe}_2)_{18}\text{PPh}_4$

$\text{Ag}_{25}(\text{SPhMe}_2)_{18}\text{PPh}_4$ was as a precursor to synthesize $\text{AuAg}_{24}(\text{SPhMe}_2)_{18}\text{PPh}_4$.^{S1,S2} About 20 mg $\text{Ag}_{25}(\text{SR})_{18}$ was dissolved in 5 ml CH_2Cl_2 and 8 μl AuClPPh_3 (~ 1 mg/200 μl DCM) was added under vigorously stirring. The reaction lasts for 4h at room temperate. The color of the reaction solution changed from reddish brown to green. The precipitate of the clusters was then dissolved in CH_2Cl_2 and crystallized in CH_2Cl_2 /hexane at room temperate for several times.

1.4 Characterization

All UV/Vis absorption spectra of nanoclusters were recorded using an Agilent 8453. Thermo gravimetric analysis (TGA) was carried out on a thermo gravimetric analyzer (DTG-60H, Shimadzu Instruments, Inc.) with 5 mg of the nanocluster in a SiO_2 pan at a heating rate of 10 K min^{-1} from 323 K to 1073 K. X-ray photoelectron spectroscopy (XPS) measurements were performed on a Thermo ESCALAB 250 configured with a mono chromated $\text{AlK}\alpha$

(1486.8 eV) 150W X-ray source, 0.5 mm circular spot size, a flood gun to counter charging effects, and the analysis chamber base pressure lower than 1×10^{-9} mbar, data were collected with FAT= 20 eV. Electrospray ionization time-of-flight mass spectrometry (ESI-TOF-MS) measurement was performed by MicrOTOF-QIII high-resolution mass spectrometer. The sample was directly infused into the chamber at 5 μ L/min.

1.5 Electrochemical measurements

Electrochemical measurements were performed with an electro chemical workstation (CHI 700E) using a Pt working electrode(diameter 0.4 mm), a Pt wire counter electrode, and a Ag wire quasi reference electrode in 0.1 MBu₄NPF₆-CH₂Cl₂. Prior to use, the working electrode was polished with 0.05 μ m Al₂O₃ slurries and then cleaned by sonication in dilute CH₃CH₂OH and nanopure water successively. The electrolyte solution was deaerated with ultra-high purity nitrogen for 30 min and blanketed under nitrogen atmosphere throughout the experimental procedure.

1.6 Theoretical method

In view of the huge amount of calculation in spectrum of the cluster, the calculation was saved by simplifying SR to SCH₃. Structural optimization and TD-DFT calculation were implemented using ORCA [S3] at the PBE0/def2-SVP level. The atom-pairwise dispersion correction with the Becke-Johnson damping scheme (D3BJ) [S4] was utilized in all calculations. In addition, the RIJCOSX [S5] approximation method was used to accelerate the calculations while introducing a very small error (usually smaller than basis set errors and much smaller than electronic-structure-method errors), in which the def2/J [S6] was used as auxiliary basis. Spectral curve data were obtained by Multiwfn software package [S7]. The full width at half maximum (FWHM) was set to 0.2 eV in spectrum profile.

Reference

- [S1] C. P. Joshi, M. S. Bootharaju, M. J. Alhilaly, O. M. Bakr, *J. Am. Chem. Soc.* 2015, **137**, 11578–11581.
- [S2] M. S. Bootharaju, C. P. Joshi, M. R. Parida, O. F. Mohammed, and O. M. Bakr, *Angew. Chem. Int. Ed.* 2016, **55**, 922-926.
- [S3] F. Neese. *Wiley Interdiscip. Rev.: Comput. Mol. Sci.* 2012, **2**, 73-78.
- [S4] (a) S. Grimme, S. Ehrlich, L. Goerigk, *J. Comput. Chem.* 2011, **32**, 1456–1465. (b) S. Grimme, J. Antony, S. Ehrlich and H. Krieg, *J. Chem. Phys.* 2010, **132**, 154104.
- [S5] (a) A. K. Dutta, F. Neese, R. Izsak, *J. Chem. Phys.* 2016, **144**, 034102. (b) G. J. Christian, F. Neese, S. F. Ye. *Inorg. Chem.* 2016, **55**, 3853-3864.
- [S6] F. Weigend, *Phys. Chem. Chem. Phys.* 2006, **8**, 1057.
- [S7] L. Tian, F. W. Chen, *J. Comput. Chem.* 2012, **33**, 580-592.

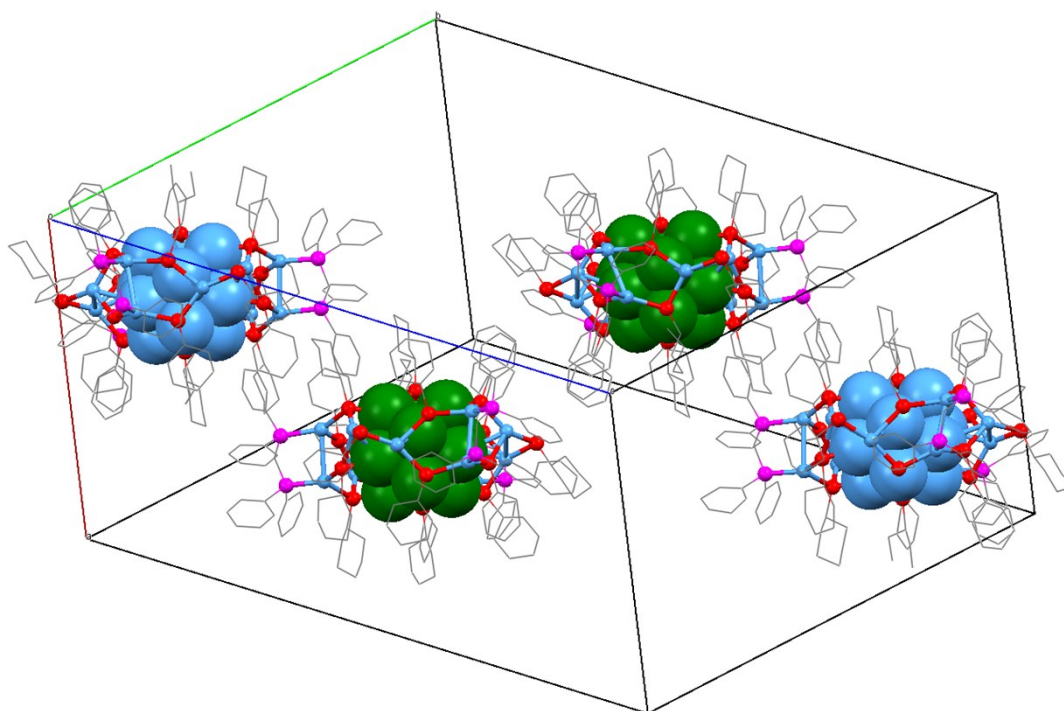


Figure S1. The parking model of $[\text{Au}_1\text{Ag}_{24}(\text{Dppm})_3(\text{SR})_{17}]^{2+}$. Color label: golden = Au; green/sky blue = Ag; red = S; purple = P.

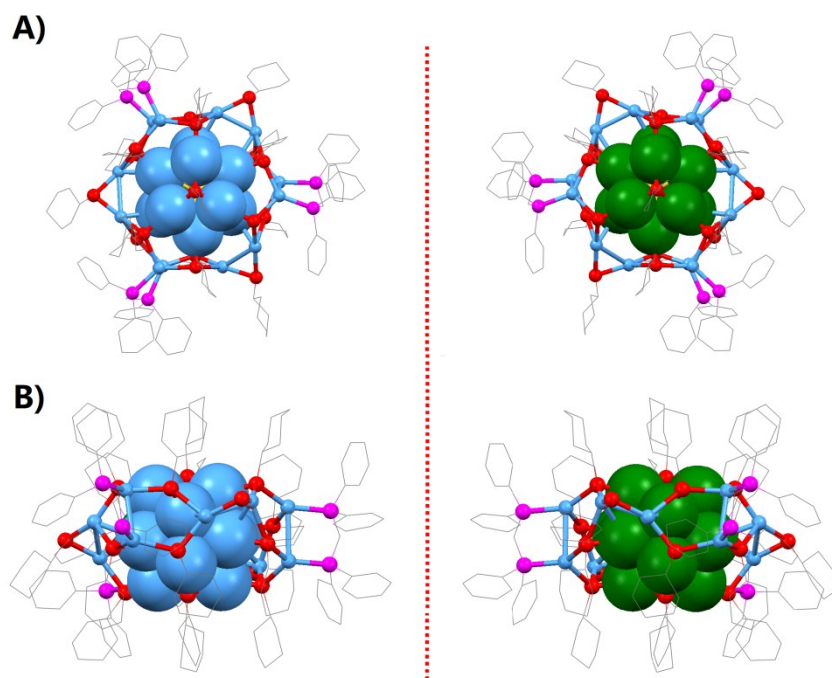


Figure S2. Two enantiomers of $[\text{Au}_1\text{Ag}_{24}(\text{Dppm})_3(\text{SR})_{17}]^{2+}$ from different perspectives. A) Top view and B) Side view. For clarity, H are omitted. Color label: golden = Au; green/sky blue = Ag; red = S; purple = P

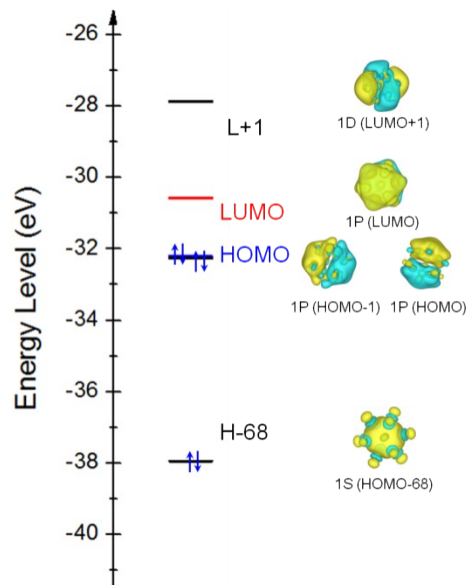


Figure S3. The kohn-sham orbitals of $[\text{Au}@\text{Ag}_{12}]^{7+}$ specie.

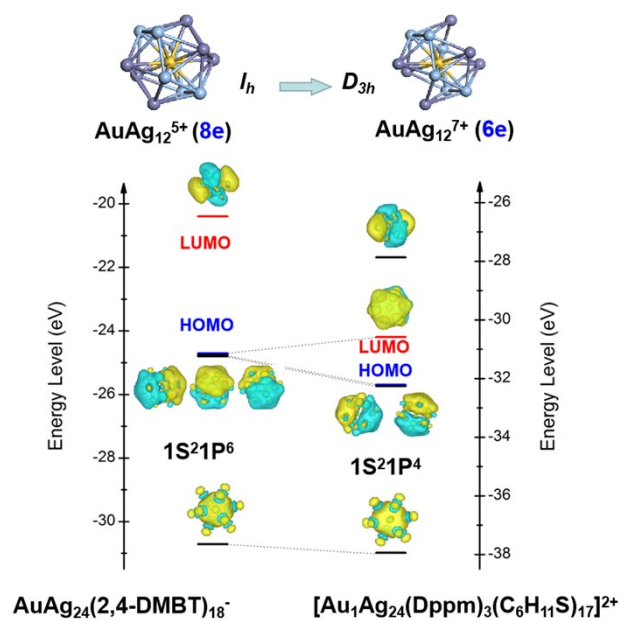


Figure S4. The kohn-sham orbitals of $[\text{Au}@\text{Ag}_{12}]^{5+}$ for $\text{AuAg}_{24}(\text{SR})_{18}^{-}$ and $[\text{Au}@\text{Ag}_{12}]^{7+}$ for $[\text{Au}_1\text{Ag}_{24}(\text{Dppm})_3(\text{SR})_{17}]^{2+}$.

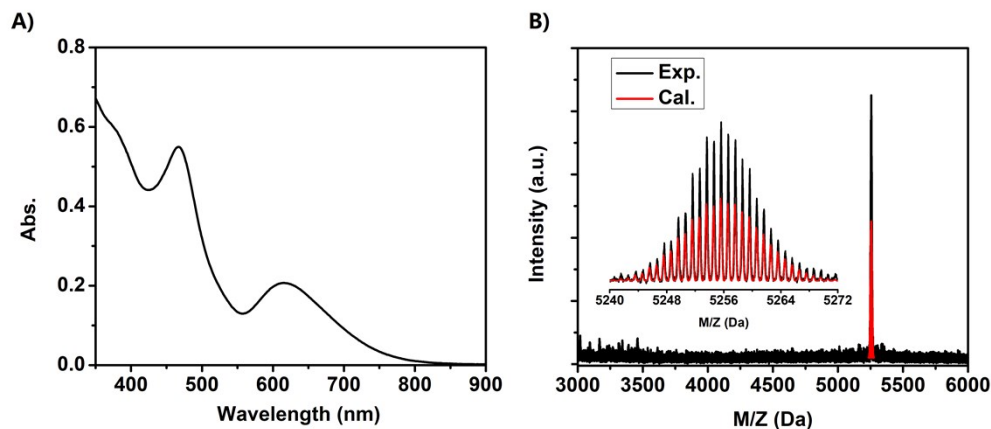


Figure S5. A) UV/vis absorption and B) ESI-MS spectra of $\text{Au}_1\text{Ag}_{24}(2,4\text{-DMBT})_{18}^-$ crystallized in $\text{CH}_2\text{Cl}_2/\text{hexane}$ at room temperature for several times.

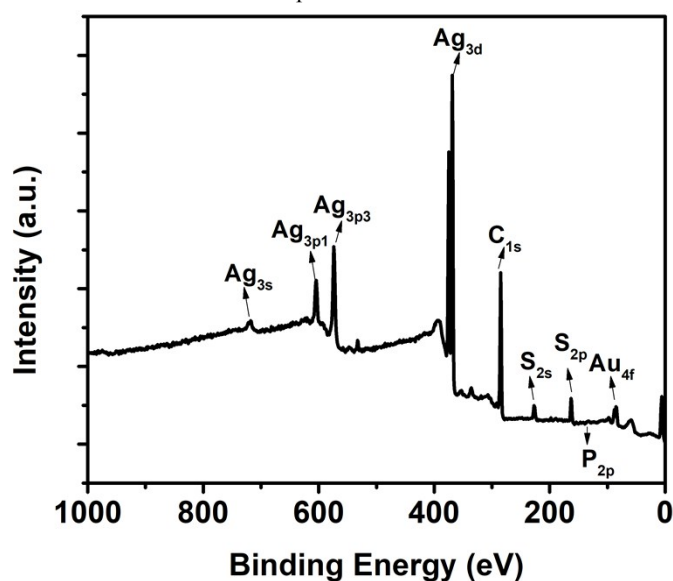


Figure S6. X-ray photoelectron spectroscopy (XPS) spectra of $\text{AuAg}_{24}(2,4\text{-DMBT})_{18}^-$.

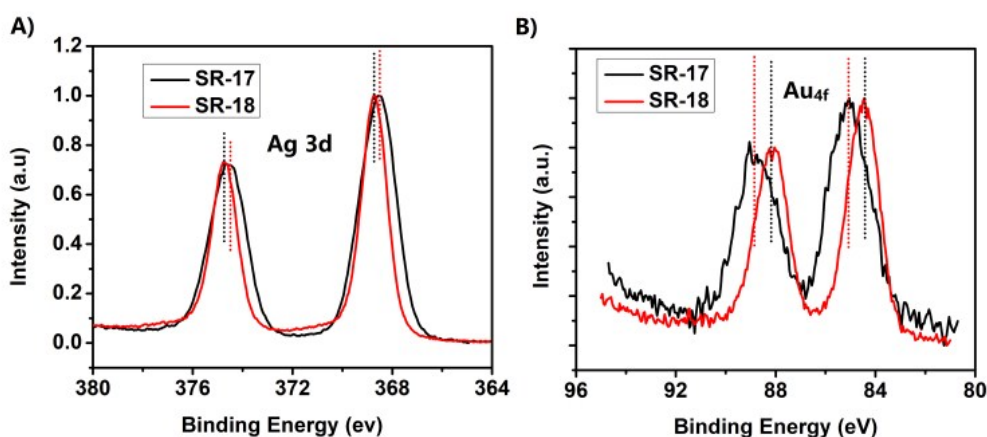


Figure S7. A) Ag 3d and B) Au 4f XPS spectra of $[\text{AuAg}_{24}(\text{Dppm})_3(\text{C}_6\text{H}_{11}\text{S})_{17}]^{2+}$ and $\text{AuAg}_{24}(2,4\text{-DMBT})_{18}^-$. Black line stands for $[\text{AuAg}_{24}(\text{Dppm})_3(\text{C}_6\text{H}_{11}\text{S})_{17}]^{2+}$ and red line stands for $\text{AuAg}_{24}(2,4\text{-DMBT})_{18}^-$.

Ag 3d binding energies (374.50 eV for Ag 3d_{3/2}, and 368.49 eV for Ag 3d_{5/2}) of $[\text{Au}_1\text{Ag}_{24}(\text{Dppm})_3(\text{C}_6\text{H}_{11}\text{S})_{17}]^{2+}$

are lower than those of the $[\text{Au}_1\text{Ag}_{24}(2,4\text{-DMBT})_{18}]^-$ (374.75 eV for Ag $3d_{3/2}$, and 368.74 eV for Ag $3d_{5/2}$). Besides, Au 4f binding energy (88.85 eV for Au $4f_{5/2}$, and 85.08 eV for Au $4f_{7/2}$) of $[\text{Au}_1\text{Ag}_{24}(\text{Dppm})_3(\text{C}_6\text{H}_{11}\text{S})_{17}]^{2+}$ are much higher than those of the $\text{AuAg}_{24}(2,4\text{-DMBT})_{18}^-$ (88.20 eV for Au $4f_{5/2}$, and 84.43 eV for Au $4f_{7/2}$). The results indicate both silver and gold are much more positive charged in $[\text{Au}_1\text{Ag}_{24}(\text{Dppm})_3(\text{C}_6\text{H}_{11}\text{S})_{17}]^{2+}$ nanocluster comparing with the $[\text{Au}_1\text{Ag}_{24}(2,4\text{-DMBT})_{18}]^-$, which might be due to the former nanocluster has two electrons missing from the latter one.

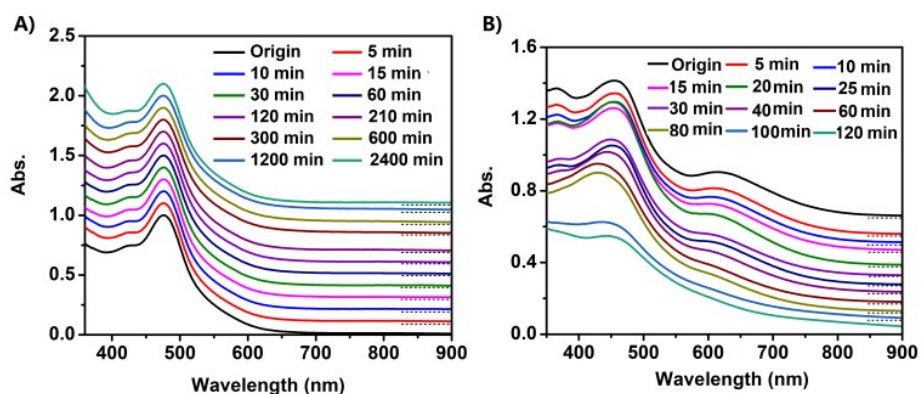


Figure. S8 UV-Vis spectra confirming the kinetic stability at 50 °C of A) $[\text{Au}_1\text{Ag}_{24}(\text{Dppm})_3(\text{SR})_{17}]^{2+}$ and $\text{Au}_1\text{Ag}_{24}(2,4\text{-DMBT})_{18}^-$.

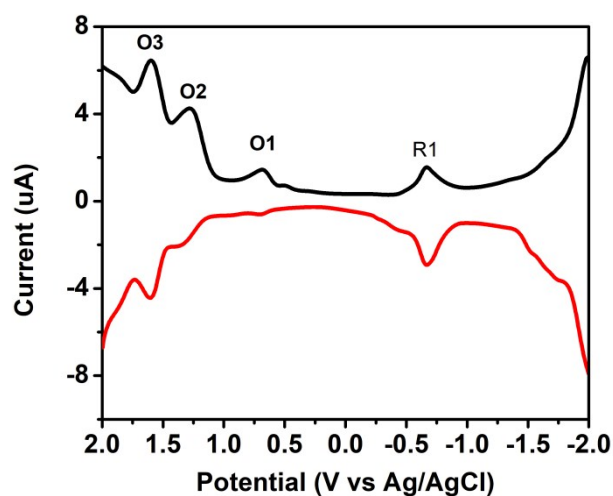
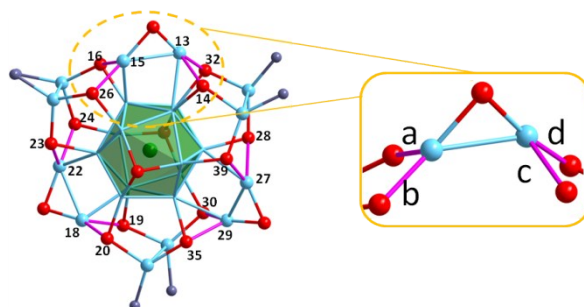


Figure S9. Differential pulse voltammogram of $[\text{Au}_1\text{Ag}_{24}(\text{Dppm})_3(\text{SR})_{17}]^{2+}$ at the low temperature environment formed in dry ice dissolved in acetonitrile.

Table S1. Bond length analysis of ligand structural units. Since there are three similar ligand units in the structure, the Ag-SR bond length in the unit is represented by a, b, c and d. Inset: The main framework of AuAg₂₄ and the serial number of Partial Ag and S atoms in the ligand shell. The C, H atoms are removed for clarity.



Structures	Bond Length (Å)					
	a (Ag15-S16)	a (Ag27-S28)	a (Ag18-S19)	b (Ag15-S26)	b (Ag27-S39)	b (Ag18-S20)
AuAg ₂₄ -exp	2.67025	2.58744	2.75946	2.45815	2.47946	2.43154
AuAg ₂₄ -tot	2.79328	2.71973	2.82526	2.50532	2.49313	2.47
AuAg ₂₄ -min	4.00237	3.06918	3.21856	2.42383	2.4485	2.4337
	c (Ag13-S14)	c (Ag29-S30)	c (Ag22-S23)	d (Ag13-S32)	d (Ag29-S35)	d (Ag22-S34)
AuAg ₂₄ -exp	2.61107	2.63422	2.78336	2.46911	2.49453	2.44946
AuAg ₂₄ -tot	2.7774	2.81919	2.83422	2.49716	2.50013	2.50254
AuAg ₂₄ -min	3.09613	3.72863	3.9317	2.44971	2.41157	2.42198

Table S2. The assignment* of peaks in UV-Vis spectra of $[\text{Au}_1\text{Ag}_{24}(\text{Dppm})_3(\text{SCH}_3)_{17}]^{2+}$.

Peak	S_n	Excitation Energies (eV)	Oscillator Strength	Attribution
α	3	1.398	0.012	HOMO \rightarrow LUMO+1 (81%)
				HOMO-1 \rightarrow LUMO+2 (16%)
	4	1.399	0.004	HOMO-1 \rightarrow LUMO+1 (40%)
				HOMO-1 \rightarrow LUMO+2 (58%)
β	9	2.399	0.190	HOMO-8 \rightarrow LUMO (7%)
				HOMO-5 \rightarrow LUMO (17%)
				HOMO-1 \rightarrow LUMO+2 (48%)
				HOMO-1 \rightarrow LUMO+1 (11%)
	15	2.469	0.170	HOMO-7 \rightarrow LUMO (7%)
				HOMO \rightarrow LUMO+3 (75%)
17	2.509	0.160	HOMO-1 \rightarrow LUMO+3 (85%)	
γ	51	3.005	0.010	HOMO-26 \rightarrow LUMO (24%)
				HOMO-25 \rightarrow LUMO (6%)
				HOMO-23 \rightarrow LUMO (6%)
				HOMO-5 \rightarrow LUMO+2 (17%)
				HOMO-4 \rightarrow LUMO+2 (8%)
				HOMO-3 \rightarrow LUMO+2 (10%)
	57	2.899	0.010	HOMO-1 \rightarrow LUMO+8 (35%)
				HOMO-1 \rightarrow LUMO+9 (24%)
				HOMO-1 \rightarrow LUMO+10 (15%)
				HOMO-1 \rightarrow LUMO+12 (7%)
58	3.050	0.020	HOMO-30 \rightarrow LUMO (10%)	
			HOMO-28 \rightarrow LUMO (56%)	
			HOMO-27 \rightarrow LUMO (5%)	

*The weight of the individual excitations are printed if larger than 0.05.

Table S3. Crystal Data and Structure Refinement for the [AuAg₂₄(Dppm)₃(SR)₁₇](BPh₄)₂

Identification code	AuAg ₂₄
Empirical formula	C ₂₂₂ H _{266.5} Ag ₂₄ AuB ₂ P ₆ S ₁₇
Formula weight	6473.14
Temperature/K	119.32
Crystal system	triclinic
Space group	P-1
a/Å	26.2814(16)
b/Å	29.5294(19)
c/Å	37.274(2)
α /°	67.902(3)
β /°	89.721(4)
γ /°	82.424(4)
Volume/Å ³	26537(3)
Z	4
$\rho_{\text{calc}}/\text{cm}^3$	1.620
μ/mm^{-1}	16.757
F(000)	12710.0
Radiation	CuK α (λ = 1.54178)
2 Θ range for data collection/°	4.352 to 129.994
Index ranges	-29 \leq h \leq 30, -34 \leq k \leq 34, -43 \leq l \leq 42
Reflections collected	370797
Independent reflections	86974 [R _{int} = 0.1720, R _{sigma} = 0.1980]
Data/restraints/parameters	86974/7563/4609
Goodness-of-fit on F ²	1.211
Final R indexes [I \geq 2 σ (I)]	R ₁ = 0.1808, wR ₂ = 0.4133
Final R indexes [all data]	R ₁ = 0.2378, wR ₂ = 0.4539
Largest diff. peak/hole / e Å ⁻³	10.40/-5.32